This paper first appeared in the ninth print edition of *Photovoltaics International* journal.

Tabbing-stringing quality control challenges

Dr. Harry Wirth, Dept. Materials Research and Applied Optics, Fraunhofer Institut für Solare Energiesysteme (ISE), Freiburg, Germany

ABSTRACT

Cell interconnection is recognized as the most critical process with respect to module production yield. If the process is not carefully controlled, cell cracking and subsequent breakage may occur. Many manufacturers promise breakage rates below 0.3-0.5% on their tabber-stringers, which applies for cells above 160-180µm thickness that are free from initial cracks. In real production, this figure strongly depends on materials, process parameters and throughput. This paper outlines some approaches that should be taken to avoid high levels of breakage in the cell interconnection process.

Automated cell interconnection on tabber-stringers

Solar cells are interconnected to a string (Fig. 1) using flat copper wires coated with solder. These ribbons are approximately 120-180µm thick and 1.5-2.4mm wide. Two-busbar cells require higher crosssections to limit serial resistance losses than three-busbar cells.

Most manufacturers still use leaded solder. Research backing the switching to leadfree options is ongoing, with the aim of preparing for compliance with future RoHS requirements for solar modules. The ribbons are applied on both sides of the solar cell, covering the silver busbars.

Flux is applied to the ribbons or the cell busbars. The solvent is then dried out. The solid flux melts during preheating, somewhat below the solder melting temperature. In its liquid, activated state, flux temporarily improves wetting by reducing oxidized top layers and by protecting the surface against new oxidation.

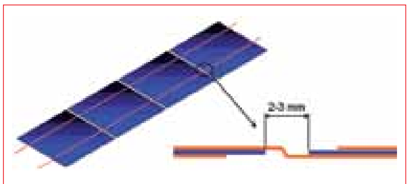

Figure 1. Cell interconnection scheme.

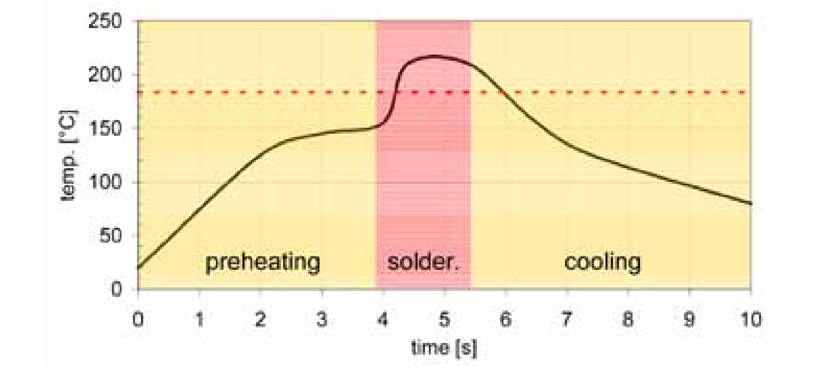

Figure 3. Schematic SnPb soldering temperature profile with preheating, soldering and cooling phase; solder is in liquid phase above dotted line.

During soldering, additional heat is applied from one side of the cell to achieve a temperature that exceeds the solder melting point by 35-40°C (Fig. 3). The molten solder must wet the busbar and completely fill the gap between ribbon and busbar.

All solder joints of one cell are formed simultaneously or in a quick sequence. During cooling, the thermal mismatch in CTE (coefficient of thermal expansion) between ribbon and cell leads to mechanical stress. The copper with a CTE of 16.5^{e-6}/°C strives to contract much stronger than silicon (2.6^{e-6}/°C). If the solder solidification point, the cooling speed, the material crosssections and the ribbon ductility are not chosen carefully, cells may crack. Decreasing cell thickness will increase the cell stress. In cells soldered on one side only, the thermomechanical stress after cooling becomes visible as bimetallic effect (Fig. 4).

With finite element modelling, the stress on a silicon wafer induced by cooling can be calculated. In Fig. 5, the red areas indicated represent tensile stress, while the blue represents compressive stress. The deep blue areas indicate compressive stress caused by the joints between the copper wire and the wafer, a result of copper's larger CTE

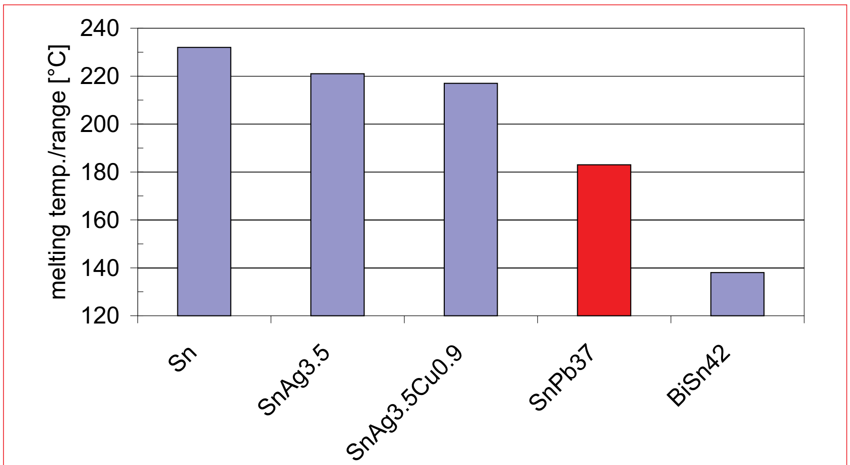

Figure 2. Melting points of eutectic solders.

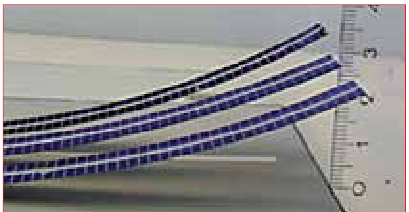

Figure 4. Stress visualization on unilateral soldered 160µm cell strips caused by CTE difference.

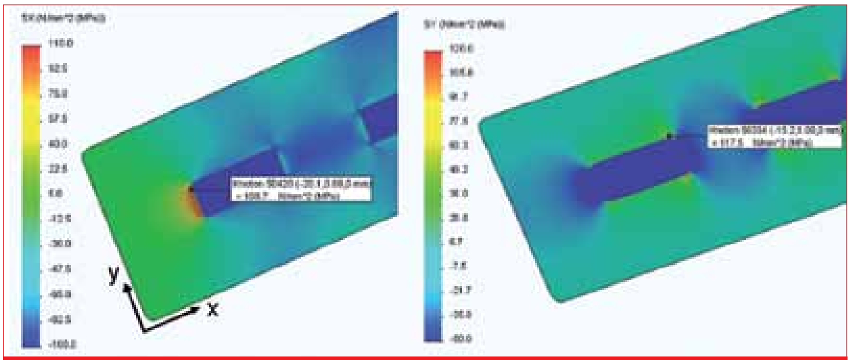

Figure 5. Calculated normal x- and y-directed stress in cell joints after cooling.

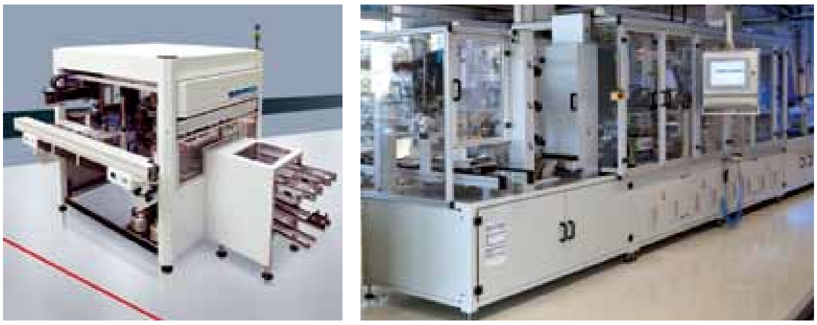

Figure 6. Tabbing unit from Schmid (left) and combined tabber-stringer from Somont.

which causes more extreme contraction than silicon. For the brittle silicon, tensile stress is critical.

Source: Somont

Figure 7. Vision system for initial cell alignment and control.

The solder joint over the busbar length may be continuous or interrupted. Interruptions longer than 15-20mm may generate series resistance losses, depending on the resistivity of the busbar.

The tabber-stringers used for fully automated cell interconnection work with a variety of heating technologies including contact, induction, resistive, lamp, hot air or laser soldering. Soldering is usually performed within a cycle time of approx. three seconds per cell on state-of-the-art machines. Automated cell interconnection is implemented as a onestep process or in two steps, with separate tabbing and stringing.

Initial cell inspection

The electric parameters of solar cells are always measured after their production, not least because STC power will eventually determine cell price. Module manufacturers usually check electric properties of incoming cells only randomly in an off-line procedure before string production.

For the module manufacturer, mechanical damage recognition in cells is a crucial task. In order to achieve safe automated handling and soldering, it is important to ensure edge integrity of the cells. Damaged edges are very likely to cause cell breakage during string and module production, leading to rejected strings, string repair or even machine down-time for cleaning. Many edge cracks will also cause power loss in the cell and ultimately in the string and module. Finally, clients may reject modules due to visible cell defects, even when they are getting the specified module power.

Visual inspection systems are used to check cell edges and busbars and to align cells for stringing (Fig. 7). A complete busbar print is required for proper soldering. Aligning cells through busbar recognition gives higher precision and handling safety than using mechanical edge contact. In Somont's Rapid and Certus stringers, the cells are aligned by servo motors during the transfer to the soldering belt, based on the vision system information.

Aside from broken edges and corners, less visible cracks inside the cell perimeter are also critical. Cracks usually extend into the cell surface, either on the emitter side, on the base, or both. A crack will nearly always increase the series resistance of a cell, depending on its length, its orientation and position with respect to the design current flow on the cell. If the crack occurred in wafer or cell production, and did not merit cell rejection, the electric damage will lead to a lower cell power classification. Cracks may also originate from transport and handling before cells enter the tabberstringer.

Even if cracks do not immediately weaken electric cell performance as specified by the cell supplier, they threaten future cell performance and durability. Mechanical loads during module production, transport, installation and operation can lead to crack growth. As soon as cell metallization is severely affected by a crack, it will increase cell series resistance and weaken cell performance. Due to the series interconnection of cells and common diode protection schemes, the weak cell will affect two strings, which usually account for one third of the PV module.

Therefore, the module producer must prevent cracked cells entering production and must ensure that the processes, especially the cell interconnection, will not produce cracks. If cracks are detected, their origin must be determined, as the processes being used may not only be revealing cell cracks, but causing them.

Small cracks pose a serious challenge

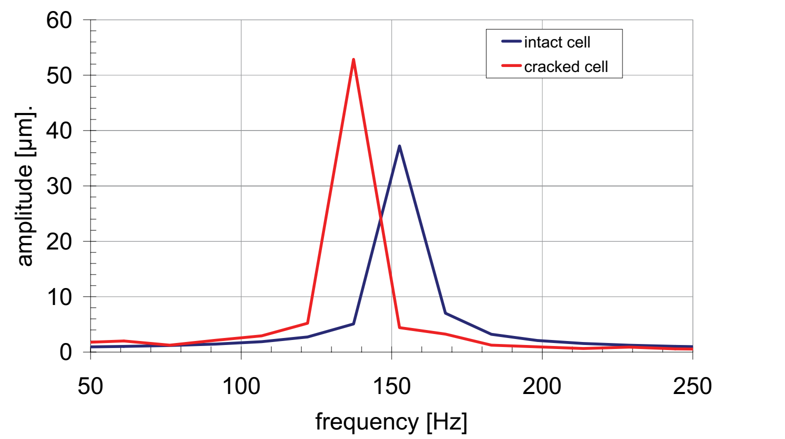

Fig. 8. Response spectrum of an intact cell and a cracked cell.

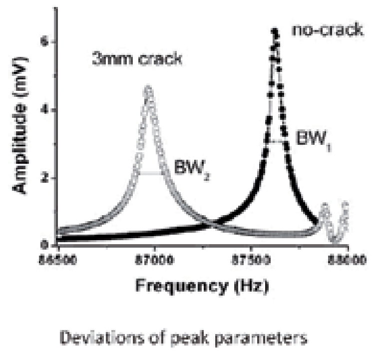

Source: RUV systems

Figure 9. Ultrasonic response spectrum of an intact and a cracked cell as recorded by the RUV crack detection system.

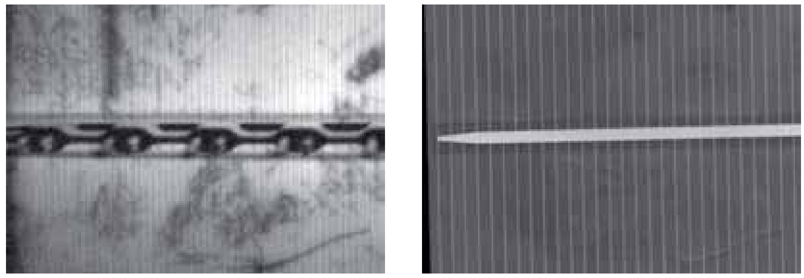

Source: GP Solar

Figure 10. EL image and contactless IR scanned image of the same cell showing several cracks.

to inline metrology, which has led to a multitude of technologies for initial crack detection (prior to soldering) being proposed. Crack length may grow if cells are bent. Longer cracks will then increase the bow of a cell under the same bending force. The approach of comparing the elastic response from two consecutive stress tests was followed in a crack testing device developed by Solarwatt; however, the device did not find its way into production lines.

Another approach comes from acoustics. Cracks may change the resonance frequency of cells subjected to sound excitation or they may introduce new frequencies in the response spectrum. Fig. 8 shows a reduction of the main resonance frequency by nearly 20Hz due to cell cracks, as recorded by a vibrometer. Some cracks also generate low-frequency noise. The measurements displayed in Fig. 8 have been performed on single tabbed cells.

RUV Systems offers a system for inline or offline crack detection based on acoustic resonance measurement [1], which uses ultrasonic frequencies, thus avoiding interference with other sound sources in the production environment. The inline implementation achieves a cycle time of three seconds.

Electroluminescence (EL) imaging has become a widely used tool for the recognition of defects in solar cells [2]. When a current flows through the cell, the recombination of electrons and holes emits radiation between 900–1400nm, peaking around 1150nm. This radiation can be registered by CCD detectors with spectral response ranging from approximately 300 to 1100 nm or by InGaAs detectors ranging from 900 to 1700nm. The latter offer better signal amplitudes, but have drawbacks in terms of lower image resolution and higher price.

Cracks appear as fine dark lines in EL images. Cracks that interrupt metallization and disconnect a region of the solar cell will appear as extended dark areas. In monocrystalline cells, cracks usually follow the crystal axis and are easily detected due to the homogeneous EL activity. In multicrystalline cells, grain boundaries and impurities render the automated detection more difficult (Fig. 10 (left)).

At present, initial EL imaging is not a common feature in automated tabber-stringers, possibly a result of the cost of inline EL implementation and the requirement of cell contacting. EL also requires a dark environment.

GP Solar recently presented a contactless IR inspection system for cells, the GP MICROD Vision, which is based on a line scanner that measures reflected IR radiation. In the reflected signal, material defects of mc silicon wafers do not show up, making the detection of cracks somewhat easier. The system measures on the fly with a belt speed of up to 400mm/s. GP Solar's crackdetection software claims very stable recognition due to the exclusion of grain boundaries and other bulk material defects.

Materials

Ribbon

The choice of an appropriate ribbon crosssection is influenced by contradicting requirements. A high cross-section is required for low serial resistance power losses, but will increase the mechanical stress on the tabbed cell; moreover, if the ribbon width exceeds the width of the cell busbar, additional shading losses are generated.

The use of ETP quality copper ensures high electric conductivity. Tin-based solder coating materials have a much lower electric conductivity than copper and will contribute little to the total conductivity. The mechanical properties of the ribbon are of huge importance to string durability from the string manufacturing all the way to module operation.

The yield strength (Rp0.2) has a direct influence on the thermomechanical stress, which is brought about by a mismatch in the coefficients of thermal expansion (CTE) of copper and silicon. The stress occurs immediately after soldering takes place, starting at the solidus temperature of the solder down to room temperature. It also occurs during module operation due to temperature variations, and, of course, in the temperature cycle test from -40°C to +85°C according to the IEC standard. Low yield strength will relieve this stress by supporting plastic deformation of the ribbon. At present, manufacturers are struggling to decrease Rp0.2 to values below 100N/mm^2, a 'softness' that is achieved by thermal annealing. In the stringer, the ribbon is cut and sometimes stretched to ensure straight alignment. This ribbon handling must ensure that yield strength is not significantly increased.

A second important ribbon specification is the elongation at fracture. Modules in operation will face deflections due to wind and snow loads, combined

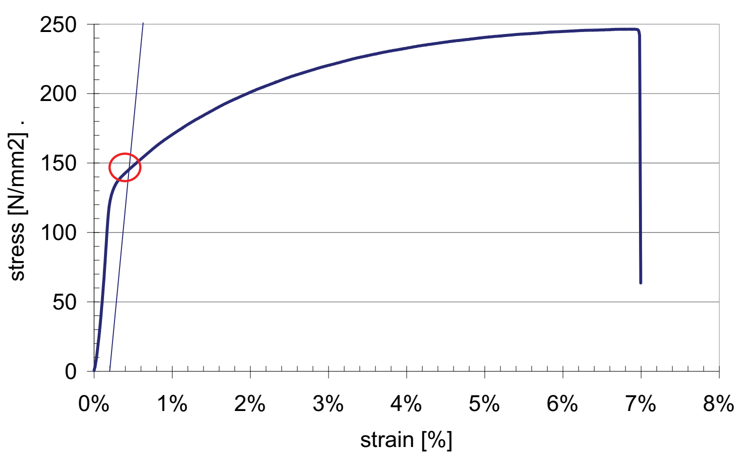

Figure 11. Stress-strain diagram of a ribbon.

PV Modules

Figure 12. Wetting angle measurement for molten solder balls on cell busbar.

with temperature changes. As a result, the ribbon sections between the cells have to resist elongation. Typical specifications can guarantee elongation values at fracture above 25%.

The measured stressstrain data in Fig. 11 indicates an Rp0.2 point at 145N/mm^2. Tensile strength Rm is just below 250N/mm^2 (without correction for reduced cross-section) and elongation at fracture only reaches 7%.

Additional parameters influencing stress behaviour include ribbon aspect ratio (height/width) and ribbon design. Current developments are focussing on ribbons with reduced CTE and ribbons with a layer structure.

The copper core of ribbons is coated by hot dipping or plating with tin-based solders. Leaded qualities include SnPb 63/37 or SnPbAg 62/36/2; lead-free qualities include Sn100, SnAg 96.5/3.5 or SnAgCu 96/3.5/0.5. Low-melting lead-free solders show various compositions of tin and bismuth. Noneutectic alloys display a melting temperature range between their solidus and liquidus points instead of a singular melting point. Solder coating should have a uniform thickness over the ribbon length that is similar on both sides and research has yielded best results with solder layers of 10-20µm.

Solderability

During soldering, the molten material must spread over the busbar surface and fill the air gap between busbar and ribbon, which requires good wetting properties to ensure occurrence at temperatures not higher than 40°C above the melting point.

The interaction between busbar surface, flux and solder is responsible for the wetting process. Wetting quality is measured by specifying the wetting angle, which can be observed by applying solder balls on cell busbars in a chamber with inert gas, as shown in Fig. 12. Small values below 30° are considered good wetting in the electronics industry, but they are difficult to achieve on solar cell metallization. Good wetting will lead to high peel forces.

For good solderability, cell storage must ensure that the top layer of oxidized silver stays thin. Otherwise, soldering temperature and flux activity have to be increased and may lead to secondary problems.

Fluxing

Cell soldering requires a no-clean, halogen-free flux that is deposited on the ribbon or on the cell busbars, usually occurring in the tabber-stringer just before soldering by using dilutions with very low solid content. The amount of flux needs to be carefully controlled, as excessive flux application contaminates the machine and the strings and may also cause adhesion problems in the laminated module. Insufficient flux may cause wetting problems during soldering, leading to incomplete joints.

Flux can be applied on the wire by transporting it through a flux bath. The Somont Certus stringer uses a flux jet technology, with optional selective fluxing on just the contact side of the ribbon. Other manufacturers favour the application of flux directly to the cell busbars.

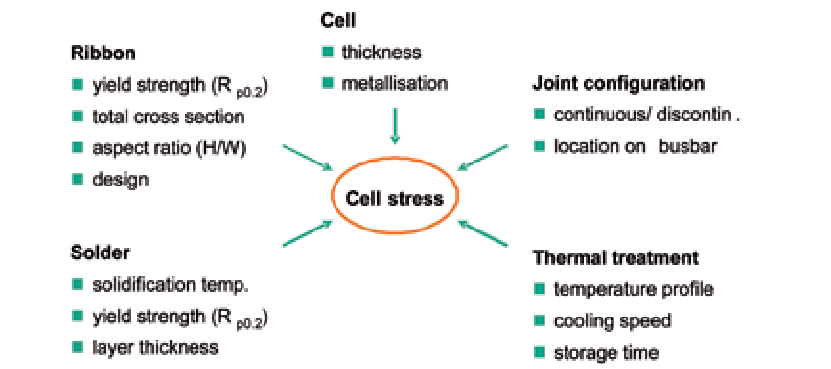

Figure 13. Cell stress parameters after solder cooling.

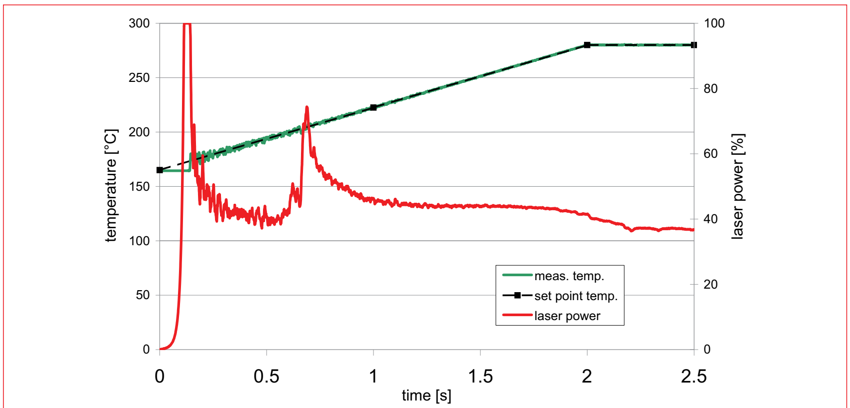

Figure 14. Laser soldering process with pyrometer control.

Critical parameters for cell stress

As a result of CTE mismatch, soldered joints start to stress the cell immediately after cooling below the solidus point of the solder [37]. After the stringer step, this stress may lead to easily audible cell cracking. A multitude of parameters influence the magnitude of the thermomechanical stress and its evolution in time, depicted by the schematic in Fig. 13. Solder and ribbon are responsible for stress relaxation by plastic deformation. Since this relaxation takes some time, the joints are at their lowest strength immediately after soldering. This is also reflected by the fact that pull tests show better results when performed some time after soldering.

Quality control during soldering

Preheating just before the soldering step ensures the proper activation of flux. The cooling phase below the solidus temperature of the solder, essential for stress relaxation, involves the counteraction of two processes. The stress induced by the thermal mismatch between silicon and metals increases as the ambient temperature is approached; conversely, stress is relaxed by plastic deformation in the copper and the solder. After soldering, a slow, controlled cooling of the solder joints is required for thermo-mechanical stress

Figure 15. The Xinspect string inspection system by Komax Solar.

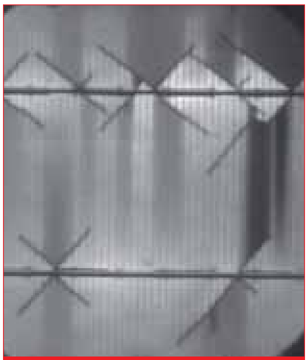

Figure 16. EL image of cell with heavy soldering-induced cracks.

relief. Preheating and cooling zones in the stringers will usually be equipped with one or more temperature control units.

During soldering, the control of the temperature profile in time and its spacial homogeneity requires great care. The time above the liquidus point should be kept short to avoid excessive diffusion. Pyrometers measure temperature contact-free and at fast rates down to 0.1ms intervals. However, their signals have to be corrected for emissivity variations. Pyrometers will only report temperature in one region of the cell if no scanning is used. Measurement on ribbons is difficult due to their low emissivity and corresponding weak radiation signal. Additionally, their emissivity may change in the course of the process.

Together with quickly responding energy sources like resistive heating, induction fields, laser beams or – to some extent – lamp irradiation, pyrometers offer the most accurate temperature control. Fig. 14 shows a perfect fit between the set temperature profile and the recorded temperature profile during a laser soldering process. Laser power (red line) has been dosed precisely to meet the specified profile.

Schmid's tabbing unit shown in the lefthand image in Fig. 6 is equipped with one pyrometer for each busbar that measures at time intervals of 5-10ms. Abnormalities in the relation between pyrometer signals and delivered power can give hints on disturbed heat transmission and may identify joint defects.

In contact soldering, the tool surface temperature is controlled at a much slower rate. Its thermal mass will hardly allow for any corrections in the course of the single soldering process, but it can ensure a uniform, reproducible heating. Care must be taken to avoid soiling on its contact surface, since this will change the heat flow.

Quality control after soldering

Inline procedures

An inline visual inspection of strings can detect broken cells or misaligned ribbons and cells. Backlight visual systems basically analyze contours and can detect cracks in the cell area only in the case of the aluminium screen-print layer being affected. Interconnection continuity and the correct polarity of cells in one string is checked using dark IV-measurement, which can give information on dark series resistance of the string.

String flashing will reveal faults that lead to power loss. Since flashing in this stage is only intended to give a comparative evaluation of subsequent strings, there is no requirement on the spectral distribution of radiation. LED flashers or other light sources may be used, as long as they provide a reasonable spatial homogeneity and reproducibility. Komax Solar offers the 'Xinspect' series of string testers that verify electrical performance by a monochromatic I-V curve measurement. The system is not integrated into the tabberstringer, but in the consecutive string layup system, shown in Fig. 15.

String-testing systems from Berger Lichttechnik feature a single flash tube for sunny-side-down use which generates a two-phased flash for the assessment of series internal resistance. A resistance

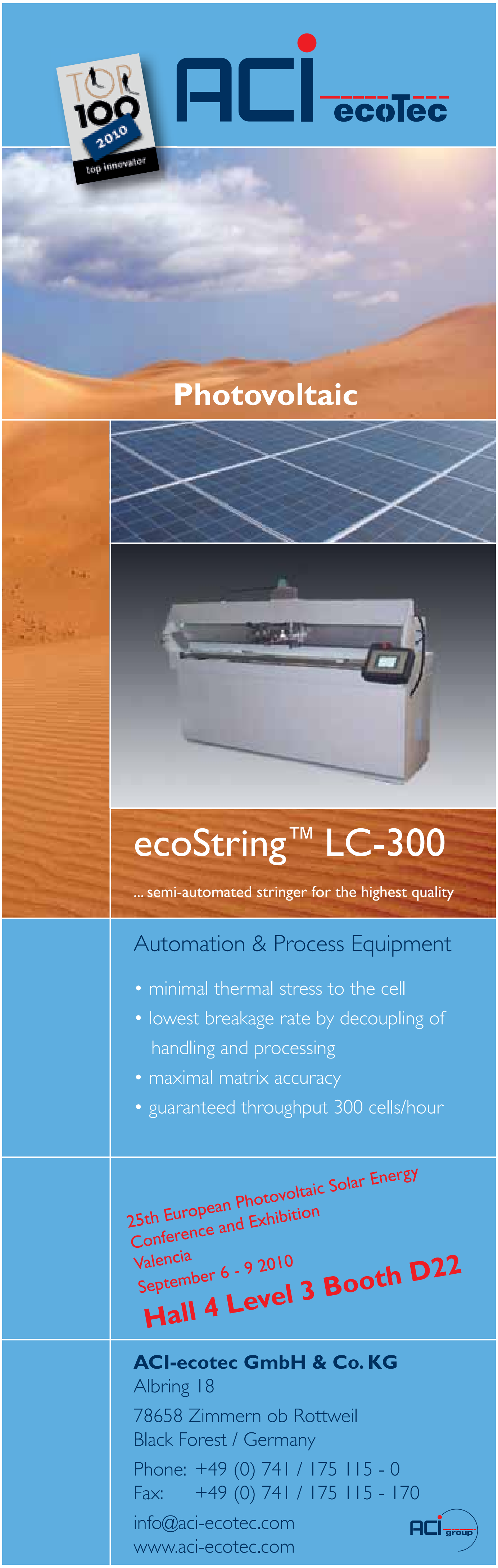

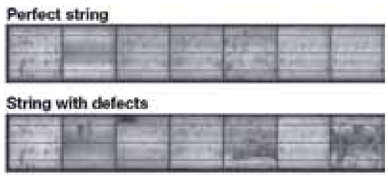

Source: Komax Solar

Figure 17. EL images of strings.

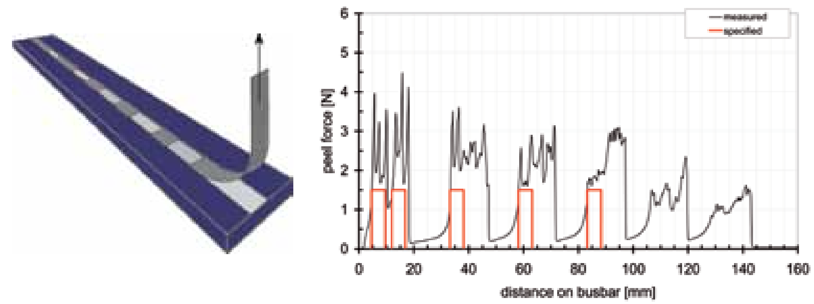

Figure 18. Example of peel test results.

increase may indicate poor contact to the ribbon or disrupted metallization, and must be addressed as it has the ability to weaken module performance.

EL imaging, as shown in Fig. 16, can show cracks in soldered cells; in this case, a very thin monocrystalline cell has been soldered to an SnAgcoated wire. Equipping the Xinspect system from Komax with an EL camera system allows inspection of strings. Fig. 17 shows an example without cracks (top, Fig. 17) and with defects (bottom, Fig. 17). Finger interruptions can cause a weaker EL signal on one side which makes the image darker. The contactless GP MICROD Vision system mentioned earlier is also intended for use in string inspection.

Offline procedures

Peel test and fracture analysis

The peel test is a widely used procedure to assess the strength of the solder joints and the fracture appearance. The EN 50461 standard, entitled "Solar cells – Datasheet information and product data for crystalline silicon solar cells" [8] requires a minimum peel force of 1N per millimetre width of the solder joint.

Generally, there are no accepted terms for the peel procedure, but the usual approach is to perform the peel test at constant speed and at a 90° peel angle, which yields a registered peel force as shown in the graph in Fig. 18.

Although this kind of peel load will not occur in module operation, the test design is used for ease of accomplishment and tradition reasons. Very thin cells and special metallizations may require different testing procedures. The peel test should be performed on automated equipment as shown in Fig. 19. Since stress relaxation after soldering is a continuous process, peel results will differ strongly if the test is performed five minutes or five hours after the process. For reliable peel results, the test is usually performed 24 hours after soldering.

Fracture appearance is as important as the recorded force. The most common fracture mechanisms include (see Fig. 20, left to right): wafer breakage, wafer chipping, paste peel-off (adhesive failure) and paste breakage (cohesive failure).

Metallography, SEM and EDX

Analytical methods from the electronics industry are used for analysis of joint integrity, composition and morphology. For example, metallographic preparation requires cutting and several polishing steps. A polished cross-section can be observed in an optical microscope (Fig. 21, left), or for better resolution, in a Scanning Electron Microscope (SEM). Fig. 21 (right, from top of image) shows the wafer, the busbar, the solder joint and the copper ribbon. Complete wetting and filling of the gap was achieved; no cracks or adhesion defects are visible. In the left image the solder layer contains dark primary lead crystallites in a grey tin matrix.

Figure 22. X-ray image of a soldered cell.

With energy-dispersive x-ray spectroscopy (EDX), chemical elements can be identified together with their distribution in the sample's crosssection. Metallographic preparation is also used to assess diffusion and phase growth processes caused by (accelerated) aging [9].

X-ray imaging

Solder joints on solar cells are mostly hidden in between the cell and the ribbon. Using a highresolution x-ray unit enables

Figure 19. Peel testing device.

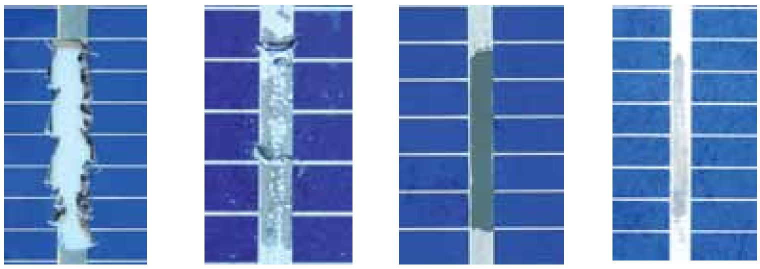

Figure 20. Peel fracture modes, left to right: wafer breakage, wafer chipping, paste peel-off (adhesive failure) and paste breakage (cohesive failure).

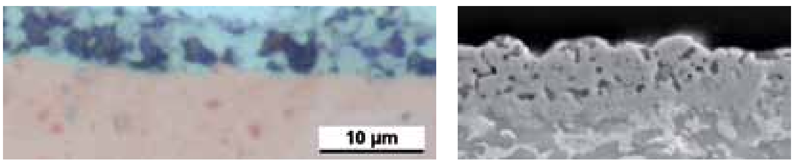

Figure 21. Metallographic images from optical microscope (left) and SEM (right).

the study of the integrity of the cell metallization and the joint homogeneity underneath the ribbons without destroying the cell. Fig. 22 shows the intersection of a finger with the busbar, where the broader p-busbar, the ribbons and the n-busbar overlie each other.

Conclusion

The process of solar cell interconnection has not yet reached the maturity evident from other industries, neither in terms of quality assurance nor in theoretical understanding. With current challenges from lead-free soldering, thinning wafers, new cell metallizations and increased line throughput, cell tabbing and stringing will have to adopt efficient metrology. The essential process parameter is the temperature profile experienced by the cell, as long as gentle handling is taken for granted. This profile will require more precise control especially during soldering and cooling. Ideally, cell integrity and functionality are assessed twice: initially and in the tabbed state. A data comparison will then reveal quality problems arising from interconnection. With respect to back contact cells, sequential tabbing and stringing needs to be replaced by simultaneous processes, for technical and economical reasons. This generates totally new challenges for quality control in cell interconnection.

References

[1] Dallas, W., Polupan, O. & Ostapenko, S. 2007, "Resonance ultrasonic vibrations for crack detection in photovoltaic silicon wafers", *Meas. Sci. Technol.*, Vol. 18, pp. 852-858.

[2] Fuyuki, T. et al. 2005, "Photographic surveying of minority carrier diffusion length in polycrystalline silicon solar cells by electroluminescence", *Appl. Phys. Lett.*, Vol. 86, 262108.

[3] Gabor, A.M. et al. 2006, "Soldering induced damage to thin Si solar cells and detection of cracked cells in modules", *21st EU PVSEC*, Dresden, Germany, pp. 2042-2047.

[4] Wiese, S. et al. 2009, "Constitutive Behaviour of Copper Ribbons used in Solar Cell Assembly Processes", *10th. Int. EuroSimE*, Delft, The Netherlands.

[5] Lalaguna, B. et al. 2008, "Evaluation of stress on cells during different interconnection processes", *23rd EU PVSEC*, Valencia, Spain.

[6] Micciche, B. & Dingle, B. 2006, "Understanding the causes for cell breakage during the cell interconnecting process – part I", *21st EU PVSEC*, Dresden, Germany.

[7] Micciche, B., Dingle, B. & Sidelinger, S. 2007, "Understanding the causes for cell breakage during the cell interconnecting process – part II", *22nd EU PVSEC*, Milan, Italy.

[8] EN 50461, 2006: '"Solar cells – Datasheet information and product data for crystalline silicon solar cells".

[9] Cuddalorepatta, G. et al. 2010, "Durability of Pbfree solder between copper interconnect and silicon in photovoltaic cells", *Prog. Photovolt. Res. Appl.*, Vol. 18, pp. 168-182.

About the Author

Dr. Harry Wirth received a diploma degree in physics in 1995 from the University of Freiburg, Germany. He earned his Ph.D. in 2000 from the Ecole Polytechnique Federale de Lausanne (EPFL). Since 2005, he has been heading the "Photovoltaic Modules" group at Fraunhofer ISE, dealing with new module concepts, cell interconnection processes and materials in the new Module Technology Center in Freiburg, Germany.

Enquiries

Dr. Harry Wirth
Fraunhofer Institute for Solar Energy Systems
Heidenhofstrasse 2
79110 Freiburg, Germany
Tel: +49 (0)761 4588 0
Fax: +49 (0)761 4588 9000
Email: info@ise.fraunhofer.de
Web: www.ise.fraunhofer.de;
www.ise-mtc.de